Proceedings of the 17th World Congress
The International Federation of Automatic Control
Seoul, Korea, July 6-11, 2008

Force Tracking Impedance Control with Variable Target Stiffness

K. Lee and M. Buss *

* *Institute of Automatic Control Engineering, Technische Universität München, Munich, 80290 Germany (E-mail: k.lee@ieee.org)*

Abstract: In this paper, a novel force tracking impedance control strategy is presented in which target stiffness is varied on-line to regulate the desired contact force without any knowledge of the environment. Humans can control contact force by adjusting their arm stiffness. The contact force can be either increased by making one's arm stiffer or decreased by reducing the arm stiffness. Furthermore, humans can keep the force tracking error within a certain range without any knowledge of environmental parameters as long as how much force they exert on the object is known to them. Analogously, the proposed control scheme achieves a contact force regulation control by adjusting the target stiffness of the impedance control. The new force tracking impedance control scheme does not require estimating environment stiffness or locations since the controller is adapted only based on the previous force tracking error between the desired and real contact force. Stability of the proposed scheme is discussed with a quadratic Lyapunov function. Extensive simulation studies with a 7 degree of freedom (DoF) robot manipulator using full arm dynamics are conducted to demonstrate the validity of the proposed scheme.

1. INTRODUCTION

As robot manipulators have evolved and their applications have been broadened, interaction (compliance) control of robot manipulators with stiff environments or objects has become a key component for the success of many manipulation tasks. Typical applications of the compliance control are deburring, assembling, grinding, and surface finishing tasks, etc. Due to the central importance of such compliant motions for robot manipulators, vast investigations have been made on this challenge over the past two decades resulting in two basic classes: hybrid position/force control, e.g. Raibert et al. (1981); Khatib. (1987), and impedance control, e.g. Hogan. (1985, 1988).

The hybrid position/force control is suitable where the environments are well structured and their geometrical information is previously known, since this strategy allows to control positions in unconstrained directions and interaction forces in constrained directions explicitly as required in many applications. However, it requires to decompose the task space of the manipulator into two subspaces: a position space and a force space corresponding to those end-effector (EEF) directions of which either the position or the interaction force is to be controlled, respectively. Therefore, it may not be a promising approach for unstructured and dynamically changing environments.

Alternatively, the impedance control strategy provides compliant manipulator motions in a unified framework for both constrained and unconstrained directions. The core of the impedance control is to regulate dynamic response of the EEF to interaction forces by establishing a suitable virtual mass-spring-damper system on the EEF. Although the impedance control scheme can provide a unified framework for both constrained and unconstrained motion control problems, an explicit interaction force control can not be achieved since it controls the interaction force indirectly by regulating the dynamic relationship between the EEF position and the interaction force. Therefore, the inability of the impedance control strategy to achieve force tracking control has been considered as a major disadvantage compared to hybrid position/force control.

As a remedy to this issue, many efforts have been made to achieve force tracking control within the impedance control framework. Some researchers introduce a sliding mode type of control based on the impedance control scheme to achieve force tracking characteristics for autonomous robots as well as teleoperation systems, see e.g. Hace et al. (1997); Cho et al. (2001); Iwasaki et al. (2003). Seraji et al. (1997) present an adaptive control scheme that generates a desired trajectory in order to regulate a desired contact force either based on the estimation of the environmental stiffness and location or without the estimation. Chan et al. (1991) proposes a variable structure control scheme based on precise environmental knowledge (stiffness and position of objects) for the robust impedance control under parametric uncertainties and external disturbances. In practical cases, however, the location and stiffness of environment are usually unknown and difficult to estimate accurately. Furthermore, an inaccurate estimation of these parameters usually leads to a large force tracking error. Jung et al. (2004) propose an adaptive impedance control in which null stiffness is assigned for the constrained motion control to guarantee a zero force tracking error combined with an adaptive control feature which makes the system robust to the uncertainties in both robot dynamics and environment parameters.

However, considering human force control capabilities when exerting a certain force on a digital scale, neither null stiffness nor variation of the desired trajectory is natural and intuitive. While one's hand is in contact with the en-

vironment, the desired trajectory of the hand or the exact knowledge of environment stiffness is not required. On the other hand, one cannot exert contact forces with null arm stiffness. Thus, suitable force tracking impedance control schemes should consider the fact that humans control the force exerted on an object by adapting their arm stiffness.

The objective of this study is to develop an intuitive and anthropomorphic force tracking control scheme within the impedance control framework. The main idea is to adapt the target stiffness of the impedance controller according to force tracking errors. Since the adaptation of the target stiffness depends only on the previous force tracking error, the knowledge of the environment stiffness is not required. Thus, the proposed force tracking impedance control is simple and robust to environmental parameter variation.

This paper is structured as follows. Section 2 reviews briefly the conventional impedance control and a novel force tracking impedance control scheme with variable stiffness is developed. Stability and force tracking errors of the proposed control scheme are discussed in Section 3. Intensive dynamic simulations are presented in Section 4 to demonstrate the efficiency of the proposed scheme for various environments including variations of the environmental parameters. Section 5 describes the conclusions drawn from this work.

2. FORCE TRACKING IMPEDANCE CONTROL

A position based impedance control is one of the most typical compliance control schemes which is briefly reviewed in the Section 2.1. It is modified with variable stiffness for a force tracking impedance control scheme in Section 2.2.

2.1 Position based impedance Control

A position based impedance control scheme consists of an inner position control loop and an outer indirect force control loop, see Fig. 1. In free space motion (zero contact forces F), the desired trajectory X_d is identical to the compliant trajectory X_c since no compliant motions are necessary. In constrained motions, however, a nonzero contact force modifies the desired trajectory in the outer impedance control loop resulting in the compliant desired trajectory, which is to be tracked by the inner motion control loop. One of the common formulations for the target impedance is

$$M\ddot{X}_{dc} + B\dot{X}_{dc} + KX_{dc} = F, \tag{1}$$

where M, B, K are $n \times n$ constant diagonal mass, damping, and stiffness matrices of the target impedance for an n-dimensional task space; F and X_{dc} denote the contact force and the corresponding desired trajectory modification $(X_d - X_c)$ by the impedance controller, respectively.

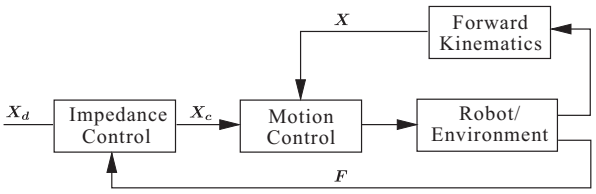

Fig. 1. Position based impedance control strategy: X_d, X_c, and X are the desired, compliant, and EEF trajectory, respectively. F is the measured force.

For simplicity, we consider a one dimensional case as shown in Fig. 2-(a), in which an EEF of a robot manipulator only just contacts with a wall without generating a contact force. It can be easily extended to the entire task space without loss of generality. In this case, (1) is reduced to

$$m\ddot{x} + b\dot{x} + k(x_d - x_c) = f. \tag{2}$$

Further, assuming good tracking performance of the inner position control loop, the compliant trajectory x_c can be reached by the EEF ($x_c = x$). Then the contact force at the steady state

$$f = k(x_d - x_c) \tag{3}$$

can be calculated. Representing the environment by a linear spring model with stiffness k_e, the contact force can be alternatively expressed by

$$f = k_e(x - x_e). \tag{4}$$

Substituting x $(= x_c)$ from (4) into (3), the steady state contact force can be rewritten as

$$f = \frac{kk_e}{k + k_e}(x_d - x_e). \tag{5}$$

Since the wall position x_e and stiffness k_e are environment parameters, (5) reveals two possible strategies to control the contact force; by tuning either 1) the desired trajectory x_d or 2) the target stiffness k. However, a desired trajectory planning that guarantees force tracking in the constrained space is not intuitive. Moreover, it can be noted that small numerical errors in the calculation of x_d will be multiplied by the resulting stiffness $(\frac{kk_e}{k+k_e})$ leading to significant force tracking errors. On the contrary, the contact force controllability can be improved by controlling the target stiffness that affects the contact force in harmonic mean fashion $(\frac{kk_e}{k+k_e})$ incorporating the environment stiffness k_e.

One interesting thing to be noticed here is negative target stiffness. When the desired trajectory x_d is set to penetrate the wall location x_e far enough, i.e., reaching x_d generates a contact force greater than the desired contact force f_d, then a positive stiffness modifies x_d in the same direction of the contact force f by (3). However, when the penetration of x_d in x_e is not deep enough, i.e., even reaching x_d can only produce a contact force f smaller than the desired force f_d, the positive stiffness will not help at all. In this case, one needs a negative stiffness which can modify the desired trajectory x_d in the opposite direction to the contact force. Fig. 2-(b) shows a modification of the desired trajectory versus target stiffness. From the above observations, a force tracking impedance control is

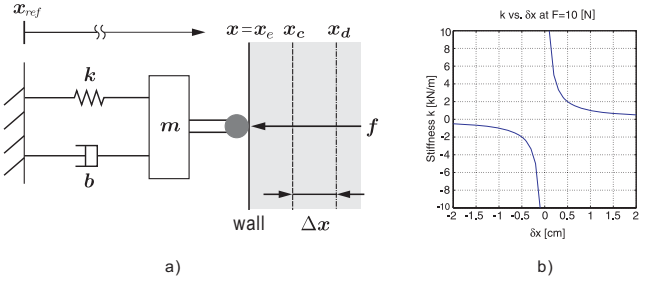

Fig. 2. Robot EEF contacting with a wall (a), and stiffness versus desired trajectory modification Δx at a given contact force $10[N]$ (b)

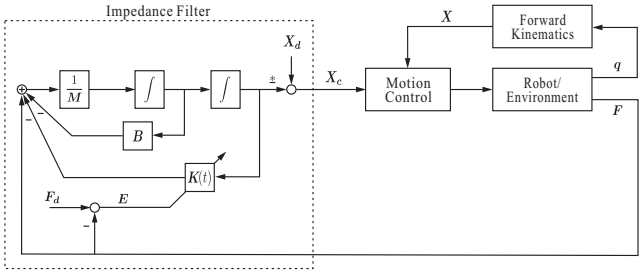

Fig. 3. Position based force tracking impedance control with variable parameters

developed in the next section with variable stiffness of the target impedance.

2.2 Impedance Control with variable stiffness

The idea is simple, intuitive, and anthropomorphically inspired. Consider a hand in contact with a wall. In order to exert more force, humans make their arm stiffer, whereas they make it softer when the contact force should be reduced. It means the arm stiffness is adapted to the difference of a desired and actual contact force. In order to imitate this human force control capability, an impedance control with variable target stiffness is proposed. The corresponding impedance equation can be written as

$$m\ddot{x}_{dc} + b\dot{x}_{dc} + k(t)x_{dc} = f. \tag{6}$$

for the one dimensional case. Thereby, b denotes a constant damping coefficient, and the stiffness $k(t)$ is adapted to force tracking errors to minimize them. The resulting force tracking impedance control scheme is illustrated in Fig. 3. Denoting the force tracking error e_f as

$$e_f = f_d - f, \tag{7}$$

the adaptation of $k(t)$ is defined as

$$k(t) = \alpha k_0 x_{dc}^{-1}, \tag{8}$$

with

$$\alpha = k_f e_f + k_v \dot{e}_f. \tag{9}$$

Thereby k_f and k_v denote a constant proportional and differential gain for the force tracking control, respectively. Substituting (6) into the force tracking error e_f, (7) can be written as

$$e_f = f_d - m\ddot{x}_{dc} - b\dot{x}_{dc} - k(t)x_{dc}. \tag{10}$$

Combining (10) with the proposed force control law (8) and (9) yields the force tracking error dynamics

$$e_f = f_d - m\ddot{x}_{dc} - b\dot{x}_{dc} - k'_f e_f - k'_v \dot{e}_f \tag{11}$$

$$\Rightarrow k'_v \dot{e}_f + (k'_f + 1)e_f = f_d - m\ddot{x}_{dc} - b\dot{x}_{dc} \tag{12}$$

with $k'_f = k_0 k_f$ and $k'_f = k_0 k_v$. Consequently, the steady state force tracking error becomes

$$e_{f,ss} = \frac{f_d}{k'_f + 1} = \frac{f_d}{k_0 k_f + 1}. \tag{13}$$

From (13), it is noted that the proposed control does not provide a zero force tracking error for none zero desired force. However, the presented method can guarantee to keep steady state force tracking error below the measurement resolution of conventional load cells. For instance, the steady state force tracking error $e_{f,ss}$ is smaller than 10^{-4} N for k_f=10^3, k_0=10^3 N/m, and f_d=100 N.

On the other hand, as mentioned in the previous section, it is not possible to obtain the desired contact force f_d with a positive target stiffness for some cases. Consider x_d does not penetrate enough in x_e such that the maximum achievable contact force f is smaller than the desired contact force f_d; $f_d > f = k_e(x_d - x_e)$. In this case, the negative target stiffness can modify the desired trajectory x_d such that the compliant trajectory x_c can further penetrate x_e such that the desired force can be achieved. The proposed scheme does not pose any limit on the sign of the target stiffness so that the time varying target stiffness $k(t)$ may have a negative sign depending on the sign of α. Since neither negative nor time varying target stiffness is widely adopted in robotics, stability of the proposed scheme is discussed in the next section.

3. STABILITY OF TIME VARYING IMPEDANCE CONTROL

The proposed impedance controller with variable target stiffness in (6) is a specific case of

$$m(t)\ddot{x}_{dc} + b(t)\dot{x}_{dc} + k(t)x_{dc} = f \tag{14}$$

which can be characterized as a second order linear time varying system. Thereby $m(t)$ and $b(t)$ are time varying positive inertia and damping coefficients, and $k(t)$ time varying stiffness. Since such systems are of significant importance in control theory many efforts have been made to provide explicit stability condition, see e.g., Harris. (1980); Rugh. (1996); Slotine. (1991); Gil. (2005). Many of those stability analyses assume slowly varying and positive definite parameters. Hence, these analyses can not apply to the proposed scheme and new stability analysis should be devised.

Consider a force regulation problem (f_d =const.) with a more general linear time varying system (14). For obtaining a force tracking control the proposed control law (6)-(9) is applied to (14). In order to analyze the stability, we define the positive scalar Lyapunov function candidate

$$V = \frac{1}{2}m\dot{x}^2 + \frac{1}{2}k_e(x - x_e)^2 + \frac{1}{2}k_n e_f^2, \tag{15}$$

where the argument t is dropped. Thereby k_n is a nominal positive stiffness which will be defined later and m is a time varying positive inertia. It is noted that the Lyapunov function candidate can be interpreted as a sum of kinetic and potential energy for the motion control and the force tracking control. Next, we assume a constant position tracking error δx in the inner motion control loop $x_c = x + \delta x$ and a constant desired trajectory x_d, (14) can be rewritten as

$$m\ddot{x} = -f_d - b\dot{x} + k'_f(e_f + 1) + k'_v \dot{e}_f. \tag{16}$$

Furthermore, due to the constant desired force f_d, the force tracking error e_f and its first time derivative can be written with a linear environment model $f = k_e(x - x_e)$ as

$$e_f = f_d - f = f_d - k_e(x - x_e), \tag{17}$$

$$\dot{e}_f = \quad -\dot{f} = -k_e\dot{x}, \tag{18}$$

for a flat environment $\dot{x}_e = 0$.
On the other hand, the time differentiation of (15) gives

$$\dot{V} = \frac{1}{2}\dot{m}\dot{x}^2 + m\ddot{x}\dot{x} + k_e(x - x_e)\dot{x} + k_n e_f \dot{e}_f, \tag{19}$$

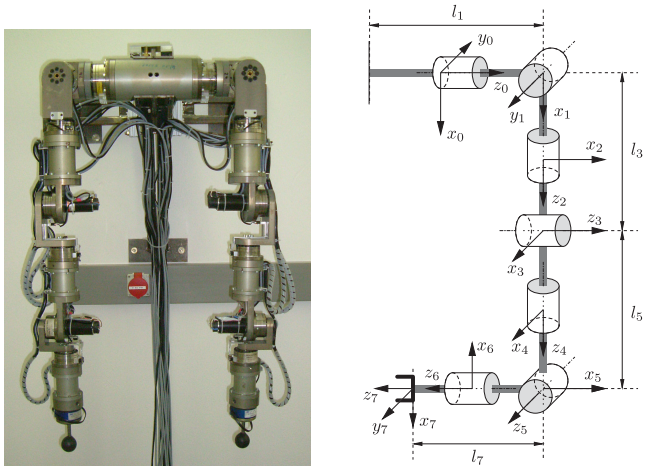

Fig. 4. Physical (left) and schematic view with link coordinate systems (right) of the 7-DoF dual arm robot

and substituting (16)-(18) into (19) yields

$$\dot{V} = \frac{1}{2}\dot{m}\dot{x}^2 - b\dot{x}^2 - k_v' k_e \dot{x}^2 + (k_f' - k_n k_e) e_f \dot{x}. \qquad (20)$$

If we now define the positive nominal stiffness k_n as

$$k_n = \frac{k_f'}{k_e}, \qquad (21)$$

then the last term on the right-hand side of (20) is canceled resulting in

$$\dot{V} = -\left(b + k_v' k_e - \frac{1}{2}\dot{m}\right)\dot{x}^2 \leq 0, \qquad (22)$$

which is negative semi-definite as long as b and $\dot{m}$ satisfy the inequality

$$2(b + k_v' k_e) \geq \dot{m}. \qquad (23)$$

Since the system is not autonomous, the invariant-set theorem is not applicable to show an asymptotic behavior of the system. However, it can be provided by invoking Barbalat's lemma. The Lyapunov function candidate V in (15) is lower bounded, since $\dot{x}$ and e_f are bounded, and $\dot{V}$ is negative semi-definite as shown above. Considering that the acceleration of the EEF is bounded in physical systems it is reasonable to conclude that

$$\ddot{V} = -\frac{1}{2}\left(2\dot{b} - \ddot{m}\right)\dot{x}^2 - 2(b + k_v' k_e - \frac{1}{2}\dot{m})\dot{x}\ddot{x} \qquad (24)$$

is also upper bounded by assuring that $(2\dot{b} - \ddot{m})$ is bounded, and it proves that the tracking error converges by resorting to Barbalat's lemma. The above stability analysis can be readily applied to (6). The stability of the proposed force tracking control scheme is thus proved.

4. SIMULATION STUDIES

The proposed force tracking impedance control presented in Sections 2 and 3 is simulated using a dual-arm redundant manipulator. The dual-arm redundant manipulator was developed at the Institute of Automatic Control Engineering (LSR) of the Technische Universität München. The physical construction and a schematic view with coordinate systems are shown in Fig. 4. Each arm consists of two spherical joints with 3 DoF at shoulder and wrist, each, and one revolute joint at the elbow, which results in

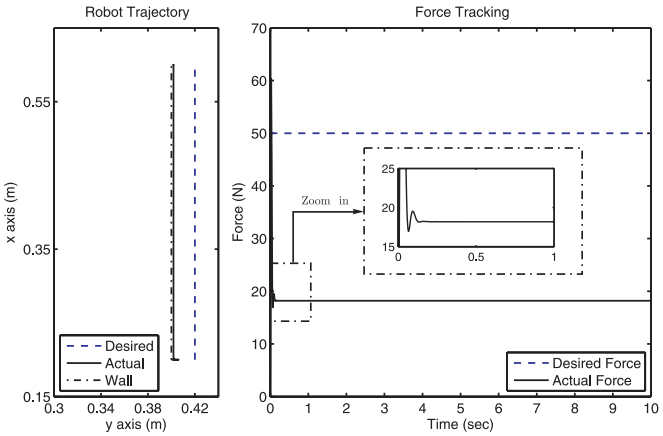

Fig. 5. Position tracking (left) and response of contact force (right) using pure impedance control; $(m, b, k) = (1, 10^2, 10^3)$, $(x_e, x_d) = (0.4, 0.42)$ m, $k_e = 10^4$ N/m

7 DoF. Both arms are built using commercially available components combined with aluminum/steel construction elements. The actuation torque is provided by DC-motors coupled with harmonic drive gears. It is equipped with six-axis JR3 force-torque sensors mounted on its EEF. The joint angles are measured by digital MR-encoders. A single arm weighs approx. 13.5 kg with a payload of 6 kg and a maximum reach of 0.86 m. In the following simulation studies the position based impedance control is employed as illustrated in Fig. 3 with full robot dynamics model and a sampling time 2 ms. The desired contact force is set to 50 N and the contact force is calculated by (4). The simulation studies consist of seven examples including variable geometries and stiffness of environment as well as a contact simulation with a conventional impedance control scheme. As a desired task, the EEF is required to keep its orientation perpendicular to a wall and move 0.4 m upward vertically while exerting 50 N to the wall. The following impedance parameters and nominal stiffness are used throughout the simulation studies: $(m, b, k_0) = (1, 10^2, 10^3)$.

Pure Impedance Control

For comparison the force tracking performance of a pure impedance control is illustrated in Fig. 5. As discussed in Section 1 and 2 the conventional impedance control regu-

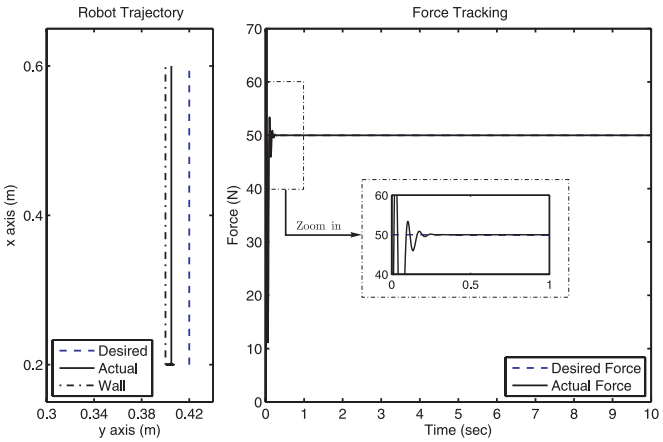

Fig. 6. Position tracking (left) and response of contact force (right); $(x_e, x_d) = (0.4, 0.42)$ m, $k_e = 10^4$ N/m

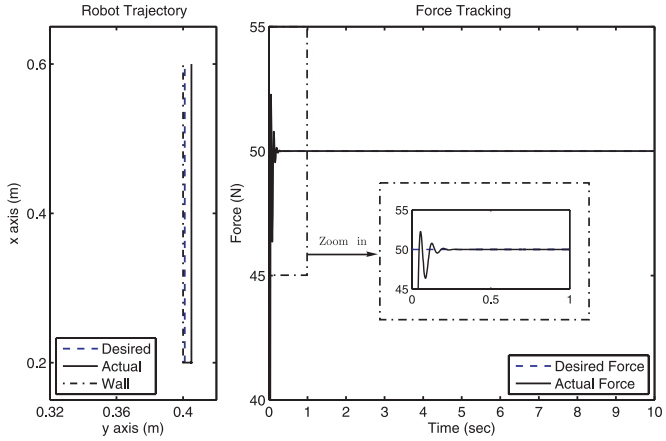

Fig. 7. Position tracking (left) and response of contact force (right); $(x_e, x_d) = (0.4, 0.401)$ m, $k_e = 10^4$ N/m

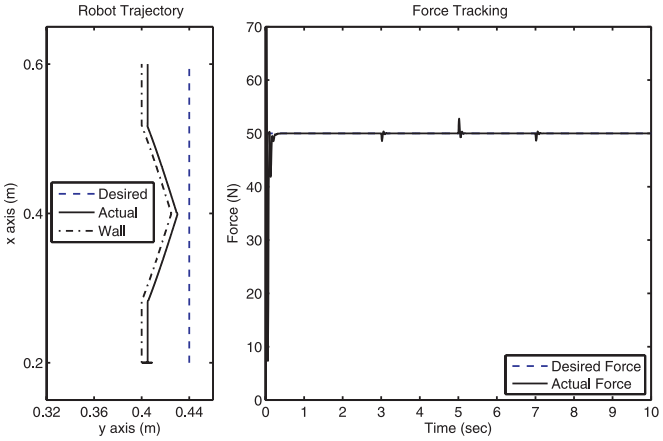

Fig. 9. Position tracking (left) and response of contact force (right); $x_d = 0.44$ m, $k_e = 10^4$ N/m

lates dynamic response of the EEF corresponding to the contact force. Therefore, it is intrinsically inappropriate for force tracking control and the force tracking error in this simulation is greater than 30 N. When the environment stiffness k_e is exactly known, although it is practically unrealistic, the difference between the desired and actual contact forces in Fig. 5 can be compensated by replanning the desired trajectory x_d.

Force Control with Constant x_e and k_e
In this simulation, the proposed scheme guarantees position tracking in unconstrained (x-) direction while the desired force is achieved in constrained (y-) direction as illustrated in Fig. 6. At the initial configuration, the EEF makes a just contact ($f = 0$) with a flat wall placed at $x_e = 0.4$ m. The force tracking control gains k_f and k_v are set to 10^3 and 26, respectively, and the target impedance parameters are selected as $M = I$, $B = 10^2 \cdot I$, and $K_0 = 10^3 \cdot I$. In this simulation, the force tracking error at the steady state $e_{f,ss}$ is identical to the force tracking error which is calculated by (13): $e_{f,ss} = \frac{f_d}{k_0 k_f + 1} < 5 \times 10^{-5}$. Since it is far smaller than the measurement resolution of conventional load cells, it can be practically treated as zero.

Force Control with Negative Stiffness
As discussed in Section 3, if the desired trajectory x_d is not placed deep enough into x_e, even reaching x_d can generate contact force f which is smaller than f_d. Since the positive target stiffness can only modify the desired trajectory in the same direction with the contact force f reducing the penetration depth $x_c - x_e$, the desired force can not be achieved. In this case, the negative stiffness modifies the desired trajectory to opposite direction of the contact force such that the compliant trajectory x_c will penetrate further into x_e. Thus, the desired contact force f_d can be achieved. Fig. 7 illustrates such kind of force tracking performance when the desired trajectory is set to $x_d = 0.401$ m which is slightly greater than $x_e = 0.4$ m. In this case, reaching x_d can only generate contact force small than the desired one ($f < f_d$). However, negligible force tracking errors could be obtained by the proposed scheme with negative stiffness and the force tracking error is identical to that of the previous simulation. Further, it is observed that the impact force during the transient phase from the free space motion to the constrained motion is much smaller than that of the previous simulation. In this simulation, the target impedance parameters are set to $M = I$, $B = 10^2 \cdot I$, and $K_0 = 10^3 \cdot I$, and the gains $k_f = 10^3$ and $k_v = 26$ for the force tracking controller.

Variable Environmental Stiffness
In this simulation, the environment stiffness k_e changes abruptly from 2×10^4 N/m to 10^4 N/m at $t = 5$ s. Since the

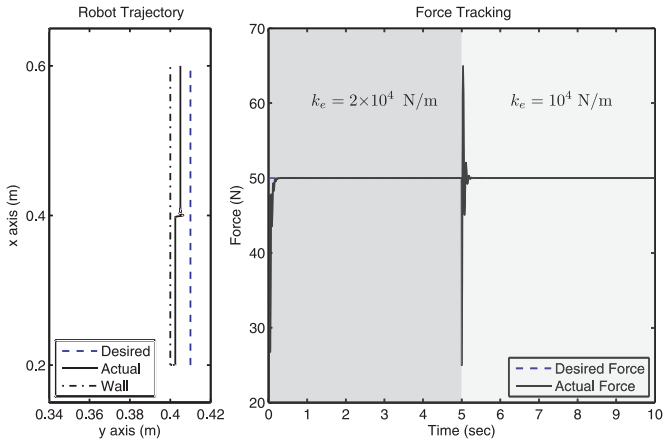

Fig. 8. Position tracking (left) and response of contact force (right); $(x_e, x_d) = (0.4, 0.41)$ m

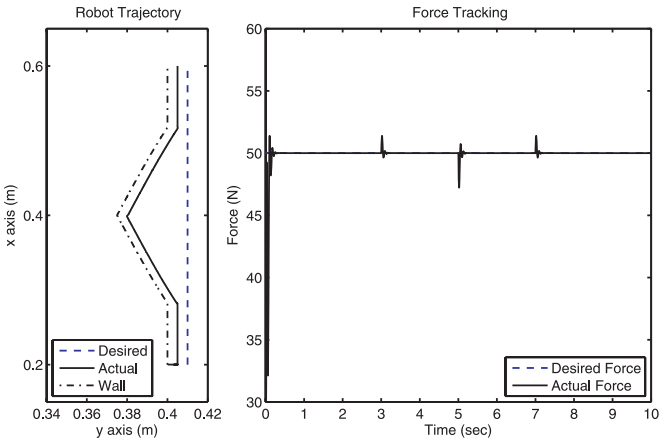

Fig. 10. Position tracking (left) and response of contact force (right); $x_d = 0.41$ m, $k_e = 10^4$ N/m

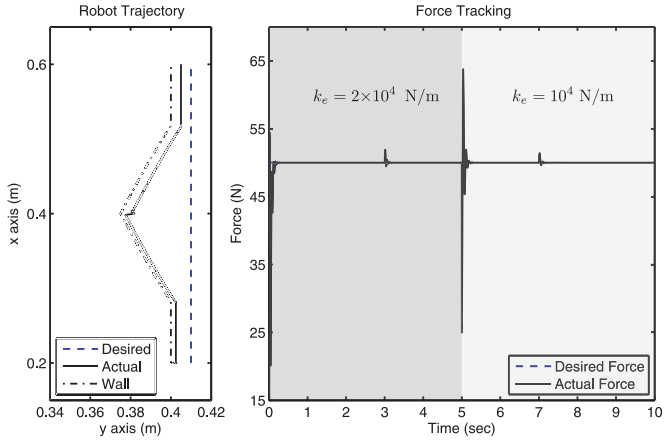

Fig. 11. Position tracking (left) and response of contact force (right); $x_d = 0.42$ m

proposed force tracking scheme adapts the target stiffness only based on the previous force tracking error, the same steady state force tracking error is achieved for both cases with different environment stiffness, see Fig. 8. The target impedance parameters are selected as $M = I$, $B = 10^2 \cdot I$, and $K_0 = 10^3 \cdot I$, and force tracking gains as $k_f = 10^3$ and $k_v = 26$. Due to the change of the environment stiffness k_e, the contact force f is perturbed at $t = 5$ s but it has settled to the desired contact force in a very short time. This simulation results show the proposed force tracking control is robust to sudden changes of the environmental stiffness while guaranteeing negligible force tracking errors.

Variable Environmental Geometry

In practical cases, the wall is not flat, hence the force tracking control should cope with surface variation of the environment. In this simulation, the proposed force tracking control scheme is applied to two different uneven environment surfaces which have a triangular type of indent and burr. The results of this simulation are shown in Fig. 9 for the triangular type of indent, and Fig. 10 for the burr type of environment surface, respectively. For both cases, it is indicated that the proposed scheme maintains the desired contact force with negligible force tracking errors throughout the task and is thus robust to variations in the geometry of the surface. Furthermore, it can be observed that the proposed force tracking control does not show any difference in steady state force tracking errors between the flat part and inclined part of the wall.

Variable Environmental Stiffness and Geometry

In this simulation, the proposed scheme is tested in the presence of both abrupt change of the environment stiffness from 2×10^4 N/m to 1×10^4 at $t = 5$ s and the triangular type of burr in the surface. The target impedance parameters are selected as $M = I$, $B = 10^2 \cdot I$, and $K_0 = 10^3 \cdot I$, and force tracking gains as $k_f = 10^3$ and $k_v = 26$. Due to the overlap of the abrupt change of the environment stiffness and geometry at $t = 5$ s, relatively large impact force is observed, but it has settled in a very short time to the desired contact force f_d and negligible steady state force tracking errors are achieved.

5. CONCLUSION

In this paper, a simple and intuitive force tracking control scheme is presented within the impedance control framework imitating human force tracking capabilities. The impedance control scheme adapts its target stiffness according to the previous force tracking error resulting in a second order linear time varying system. The proposed control scheme utilizes even negative stiffness to achieve force tracking control. Stability analysis is given for more general second order linear time varying systems where variable target inertia, damping, and stiffness are employed. Extensive simulations have been conducted for various situations including uneven environment surfaces and abrupt changes of environment stiffness. Simulation results prove the force tracking capability of the proposed control scheme for various situations without knowing the environment stiffness.

REFERENCES

M. Raibert and J. Craig. Hybrid Position/Force Control of Manipulators. *ASME J. of Dyn. Sys. Meas. Control*, 102(2), 126-133, 1981.

O. Khatib. A Unified Approach for Motion and Force Control of Robotic Manipulators. *IEEE J. Robot. Automat*, 3(1), 43-53, 1987.

N. Hogan. Impedance Control: An Approach to Manipulator. *ASME J. of Dyn. Sys. Meas. Control*, 107(1), 1-24, 1985.

N. Hogan. On the Stability of Manipulators Performing Contact Tasks. *IEEE J. of Robot. Automat.*, 4(6), 677-686, 1988.

T. Lasky and T. Hsia. On Force-Tracking Impedance Control of Robot Manipulators. *Proc. IEEE Int. Conf. Robot. and Automat*, Los Alamitos, CA, 274-280, 1991.

H.-C. Cho, J.-H. Park, K.-H. Kim, and J.-O. Park. Sliding-Mode-Based Impedance Controller for Bilateral Teleoperation under Varying Time-Delay. *Proc. IEEE Int. Conf. Robot. and Automat*, Seoul, Korea, 21-26, 2001.

M. Iwasaki, N. Tsujiuchi, and T. Koizumi. Adaptive force control for unknown Environment using sliding mode controller with variable hyperplane. *JSME Int. J. Series C, Mech. Syst. machine elements and manufacturing*, 46(3), 967-972, 2003.

Chan. S. et al. Robust Impedance Control of Robot Manipulators. *Int. J. of Robot. Automat.*, 6(4), CA, 220-227, 1991.

H. Seraji and R. Colbaugh. Force Tracking in Impedance Control. *Int. J. of Robotic Research*, 16(1), 97-117, 1997.

S. Jung, T.C. Hsia, and R.G. Bonitz Force Tracking Impedance Control of Robot Manipulators under Unknown Environment. *IEEE. Trac. Control System Techn.*, 12(3), 474-483, 2004.

A. Hace, S. Uran, K. Jezernik, and B. Curk. Robust Sliding Mode Based Impedance Control. *Proc. IEEE Int. Conf. Intell. Engnrg. Sys.*, 77-82, 1997.

C. J. Harris and J. F. Miles. Stability of Linear Systems. New York, Academic Press, 1980.

W. J. Rugh. Linear System Theory. Upper Saddle River, New Jersey, Prentice Hall, 1996.

M. I. Gil. Stability of Linear Systems Governed by Second Order Vector Differential Equations. *Int. Journal of Control*, 534-536, 78(7), 2005.

J. J. Slotine and W. Li. Applied Nonlinear Control. Englewood Cliffs, New Jersy, Prentice Hall, 1991.